Failure mode prediction for composite structural insulated panels with MgO board facings

Cite as: AIP Conference Proceedings **1922**, 050004 (2018); https://doi.org/10.1063/1.5019058
Published Online: 08 January 2018

Łukasz Smakosz, and Ireneusz Kreja

Failure Mode Prediction for Composite Structural Insulated Panels with MgO Board Facings

Łukasz Smakosz[1, a)] and Ireneusz Kreja[1, b)]

[1]*Faculty of Civil and Environmental Engineering, Gdańsk University of Technology*
Narutowicza 11/12, 80-233 Gdańsk, Poland

[a)]*Corresponding author: lukasz.smakosz@pg.edu.pl*
[b)]*ireneusz.kreja@pg.edu.pl*

Abstract. Sandwich panels are readily used in civil engineering due to their high strength to weight ratio and the ease and speed of assembly. The idea of a sandwich section is to combine thin and durable facings with a light-weight core and the choice of materials used allows obtaining the desired behaviour. Panels in consideration consist of MgO (magnesium oxide) board facings and expanded polystyrene core and are characterized by immunity to biological corrosion, a high thermal insulation and a relatively low impact on environment. Customizing the range of panels to meet market needs requires frequent size changes, leading to different failure modes, which are identified in a series of costly full-scale laboratory tests. A nonlinear numerical model was created with a use of a commercial ABAQUS code and a user-defined procedure, which is able to reproduce observed failure mechanisms; its parameters were established on the basis of small-scale tests and numerical experiments. The model was validated by a comparison with the results of the full-scale bending and compression tests. The results obtained were in satisfactory agreement with the test data.

INTRODUCTION

Composite materials allow obtaining any desired material properties depending on components used, their proportions and the type of connection between them. The possibility of obtaining low weight combined with high strength is the reason why composites are very attractive not only in transport industry, but also in civil engineering. Reducing the weight of building materials widens the scope of their application and enables more efficient and less costly transportation and structure assembly. That is why considerable effort is put to reduce bulk density of traditional materials by combining them, for example, with structural foams and fibre reinforcements. However, this also introduces complex interactions between material phases which may lead to lowered strength and influence different material properties, such as thermal insulation or water absorption, in unpredictable ways. This is why every change in composite component configuration needs to be subjected to extensive experimental studies [1].

Sandwich structures exemplify this notion by combining two materials with different qualities – a light-weight, thick core sandwiched between two high-strength, durable and thin facings, joined together by an adhesive of a sufficient strength. Resulting cross-section acts in a similar fashion as an I-beam, with facings acting as flanges and a core playing the role of a web [2]. Sandwich panel is a low-weight prefabricated product ready for an immediate assembly, which makes it easy to handle, transport and embed in the structure; it is also characterised by water impermeability, improved thermal properties and a relatively good bearing capacity. These advantages are the main reason why it is widely used in the building industry [3–13]. The most common types of panels used in civil engineering are composed of steel or aluminium facings and a polyurethane or expanded polystyrene foam core. Due to complexity of layer interactions even these widespread combinations of materials are of a great interest to researchers in terms of geometry optimisation (length, relative layer thickness, facing geometry) [3, 4, 14], localised load effects and varied support conditions [4–7], the influence of openings [8] or submission to extreme loads (windborne debris, explosions) [10, 11].

Computer Methods in Mechanics (CMM2017)
AIP Conf. Proc. 1922, 050004-1–050004-10; https://doi.org/10.1063/1.5019058
Published by AIP Publishing. 978-0-7354-1614-7/$30.00

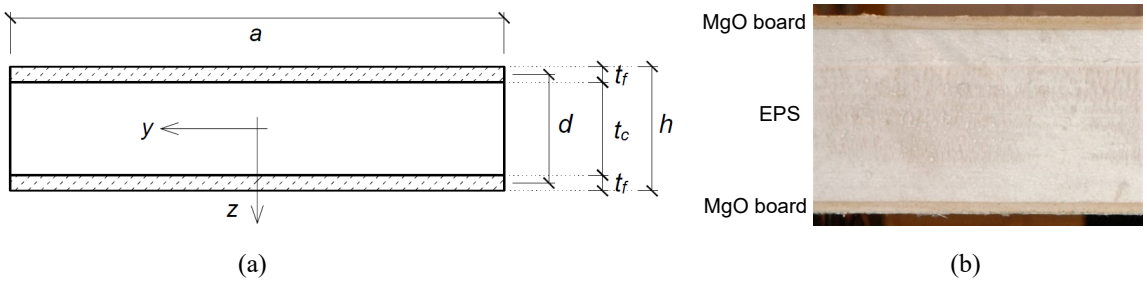

(a) (b)

FIGURE 1. Analysed CSIP's cross-section: (a) scheme with dimensions (in mm): a=1000, t_f=11, t_c=152, d=163, h=174, (b) layer view

Exchanging thin metal facings with relatively thicker, wood-based ones and using a foam core of a significant thickness created a sandwich panel variation called the Structural Insulated Panel (SIP). SIPs retain all previously mentioned advantages of standard sandwich panels and because they are less prone to local failure modes, due to thicker facings, they can take part in carrying structural loads. This type of panel can be used for floors, roofs and outer and inner walls of public and residential buildings. It can also provide sufficient thermal insulation even in extreme climates [15].

The Composite Structural Insulated Panel (CSIP) is a direct development of this idea. CSIP's facings are made of composite materials which make it considerably stronger, immune to biological corrosion and more durable to weather conditions. Such desirable improvements, in comparison to traditional SIPs, make CSIPs a very attractive alternative with a broader field of applications [16–21]. Increased strength of this type of sandwich makes it a viable option even in bridge structures [22–24].

The report describes a specific type of CSIPs with magnesium oxide board facings reinforced with fiberglass and an expanded polystyrene core (Fig. 1), bound together by a polyurethane adhesive. The EPS foam is a well-known insulating material but the MgO board is a novel solution, which provides an array of characteristics highly desirable in sandwich structures, such as high strength, immunity to biological and chemical corrosion, resistance to fire and low water absorption. This is a relatively new product and it requires adjustments in its assortment to meet market needs, which leads to frequent changes in its dimensions: length, width, and layers' thickness. Due to the complex nature of layered structures each such change requires a cycle of costly laboratory tests on full-scale panels. In order to reduce these costs a reliable tool is required, one that is able to predict the behaviour and failure modes of panels of different geometries subjected to different types of loads. In order to create such a tool, an extensive series of laboratory tests was performed and results obtained were used to develop a numerical model within commercial ABAQUS software framework [25]. The present study concerns mechanical performance of analysed CSIPs but there has also been a parallel research considering its acoustic properties [26].

EXPERIMENTAL ANALYSIS

In order to gain better understanding of analysed CSIPs and to obtain experimental data, necessary for numerical model creation and validation, two types of laboratory test cycles were performed: on small samples and full-scale panels.

In small-scale laboratory tests mechanical properties of constituent materials were measured, failure modes of samples of different geometries and layer arrangements subjected to different loadings were identified, and important physical phenomena were distinguished [27]. In all cases displacement control was used with continuous recording of traverse displacement and resulting reaction force. All small-scale test stands are presented in Fig. 2.

Full-scale tests on wall-panels of two different lengths were performed. Three edgewise compression tests with different eccentricities ($e = 0$, $e = d/6$, $e = d/3$) were performed on 2.75 m long CSIPs (Fig. 3a), and flexure caused by a set of four distributed line-loads was performed twice on 2.5 m long panels (Fig. 4a). In both cases panel cross-sections were consistent with scheme presented in Fig. 1a. The tests allowed recognizing CSIP's bearing capacity and failure modes corresponding to typical loads and to observe similarities and differences in behaviour of samples and panels [27, 28]. Displacement control was used in all of these tests as well, this time however displacements and local strains were measured in multiple points on top and bottom surfaces (Fig. 3b, c, Fig. 4b, c).

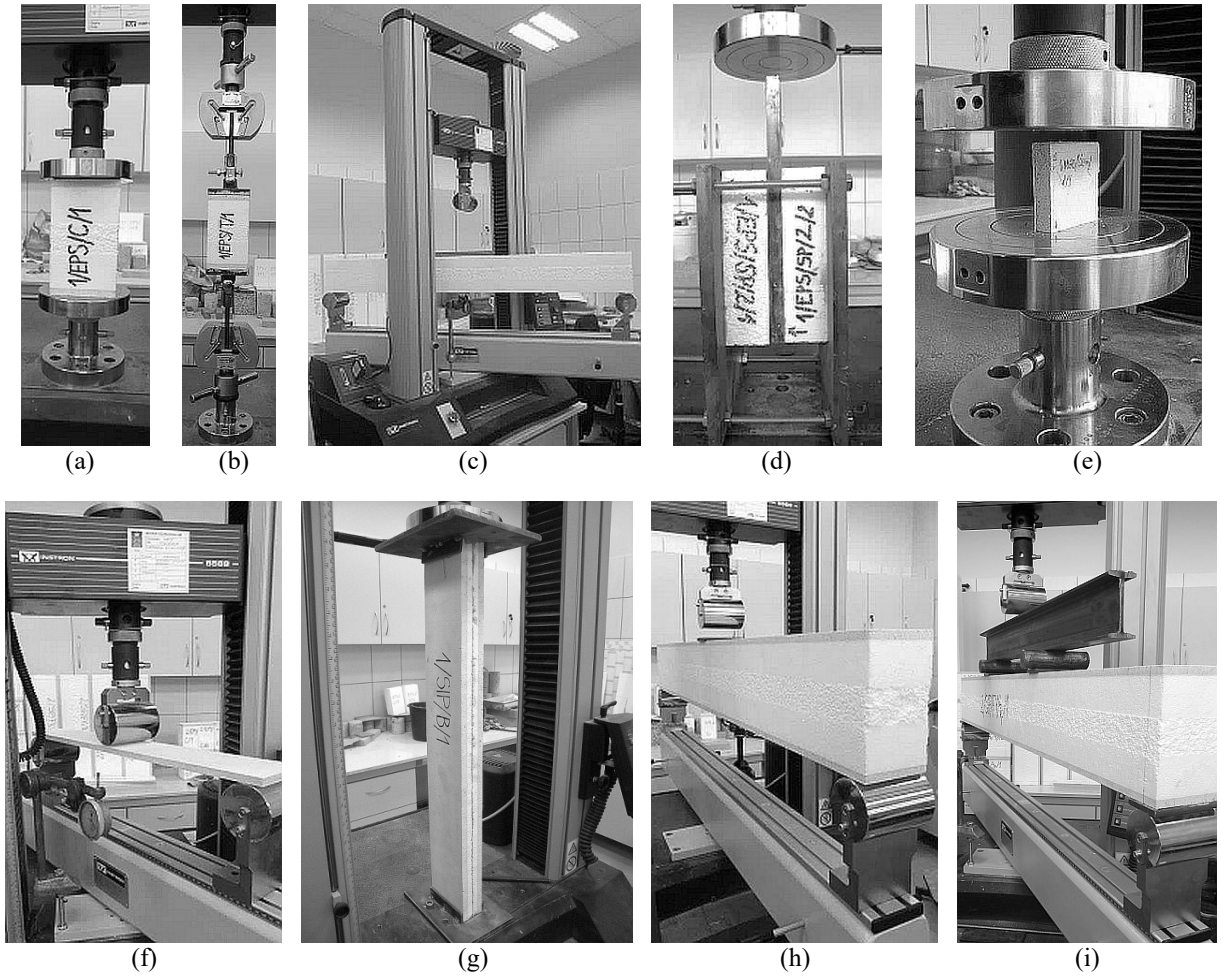

FIGURE 2. Small-scale test stands: (a) EPS compression, (b) EPS tension, (c) EPS bending, (d) EPS shear, (e) MgO board compression, (f) MgO board bending, (g) CSIP sample compression, (h) CSIP beam 3-p. bending, (i) CSIP beam 4-p. bending

FEM MODEL DESCRIPTION

Growing popularity of sandwich structures led to numerical implementation of shell theory formulations appropriate for these kinds of structures [29–35]. However, since the FEM model has to be able to predict localised failure modes, core was modelled with solid elements, based on similar research [5–11, 22–24]. Due to significant thickness of MgO board the facings were discretised with solid elements as well. Moreover, plane stress state was assumed in case of both full-scale tests and 4-node solid elements with a reduced integration and hourglass control (CPS4R) were used in the simulations. Perfect bond between facings and core was assumed. The supports and loading profiles were substituted with rigid body wire sections (R2D2) and a low friction contact was used between the rigid parts and the sample. Pinned boundary conditions were created at a single reference point assigned to each rigid profile. Displacement control was used in compression and force control in bending simulations.

Material models of analysed CSIP's layers were based on small-scale tests results. The behaviour of tested samples showed, that material nonlinearity of both, the core and facings has to be taken into account. For this purpose the Drucker-Prager yield function, with separate sets of parameters for different layers, was used [27, 28, 36]. Trial FE analyses indicated that the low stiffness of the core leads to significant deformations and so geometric nonlinearity has been taken into account as well. Importance of nonlinear approach has been also reported in recent research [19, 21, 35]. All tested samples have lost their load-bearing capacity with the initiation of damage, so failure was modelled by ductile damage initiation criterion only, without defining damage evolution behaviour.

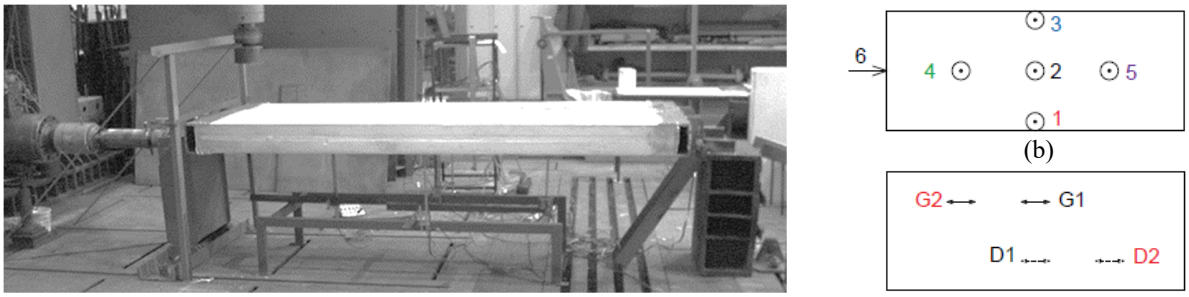

FIGURE 3. Full-scale CSIP compression test stand: (a) view, (b) displacement sensors, (c) strain gauges

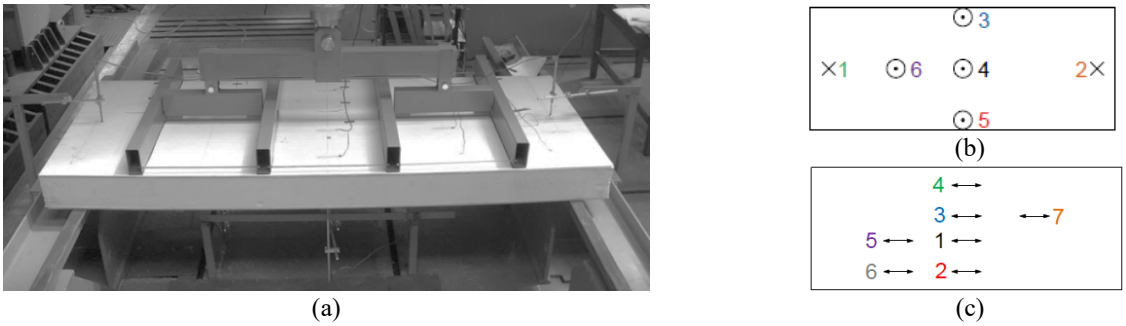

FIGURE 4. Full-scale CSIP bending test stand: (a) view, (b) displacement sensors, (c) strain gauges

Some material properties for elastic and plastic range were obtained directly from the experimental data; some were identified in a series of numerical simulations carried out in such a way to obtain satisfactory consistency with results of 15 different small-scale tests, total number combining tests presented in Fig. 2 and their geometrically varied versions (different spans or heights). Damage initiation criteria parameters were obtained as results from abovementioned simulations, corresponding to fracture loads of individual samples. Due to a large dispersion of MgO board strength properties [27], two sets of parameters were defined, corresponding to a lower and an upper limit (Tab. 1). Because EPS material property values are strongly dependent on its density [12, 14], three separate material descriptions were defined corresponding to different EPS densities recorded in laboratory tests (Tab. 1). A strengthening was assumed in a 1 mm thick strip of facing adjacent to the core, which activates conditionally during tension, and prevents premature facing failure due to stress concentrations.

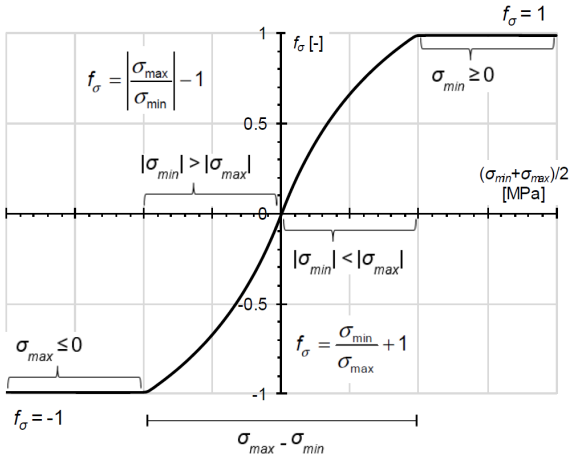

FIGURE 5. State variable f_σ value definition; σ_{min}, σ_{max} – extreme stress tensor eigenvalues

TABLE 1. Material parameter values for elastic range and hardening; f_σ – state variable, E – modulus of elasticity, ν – Poisson's number, σ_{y0} – yield stress, E_p – hardening modulus

material	f_σ [-]	E [MPa]	ν [-]	σ_{y0} [MPa]	E_p [MPa]
MgO board min	-1	2430	0.18	5.0	1600
	1	5750	0.18	4.8	2800
MgO board max	-1	3886	0.18	18.2	1600
	1	8040	0.18	6.1	1800
EPS 21 kg/m^3	-1	6.8	0.12	0.10	0.2
	0	–	–	0.09	8.0
	1	10.5	0.12	0.16	10.0
EPS 19 kg/m^3	-1	5.4	0.11	0.09	0.2
	0	–	–	0.08	7.5
	1	9.2	0.11	0.15	9.2
EPS 15 kg/m^3	-1	5.0	0.09	0.07	0.2
	0	–	–	0.07	7.3
	1	7.2	0.09	0.12	8.1

It was observed that material behaviour is strongly dependent on the stress state, both in case of core and facings, therefore a user-defined procedure had to be developed [28, 36]. The procedure produces, in every increment, at every integration point, a state variable f_σ which assumes values from –1 to 1, corresponding to states of biaxial compression and biaxial tension respectively, depending on extreme stress tensor eigenvalues (Fig. 5). Different sets of material properties assigned to selected values of f_σ were prepared for the elastic range, the plastic range and the failure initiation criterion. The most important of these values are presented in Tab. 1.

RESULTS COMPARISON

The final model was validated by a comparison with the results of full-scale bending and compression tests. Two CSIPs were subjected to four equally distanced line loads of equal intensity (Fig. 4a) [27, 28]. The comparison of the vertical deflection in the mid-span obtained from laboratory tests and numerical simulations is shown in Fig. 6a. The numerical model reflects general character of the experimental curves very well, but different sets of failure criterion parameters in tension were obtained for small-scale bending of MgO board, CSIP samples and full-scale panel. Failure initiation properties in the facing tension obtained for different samples are compared with small-scale MgO board bending experimental data in Fig. 10. Failure of full-scale panel corresponds well with the proportionality limit of MgO board sample and this value should be used instead of small-scale facing's limit strength.

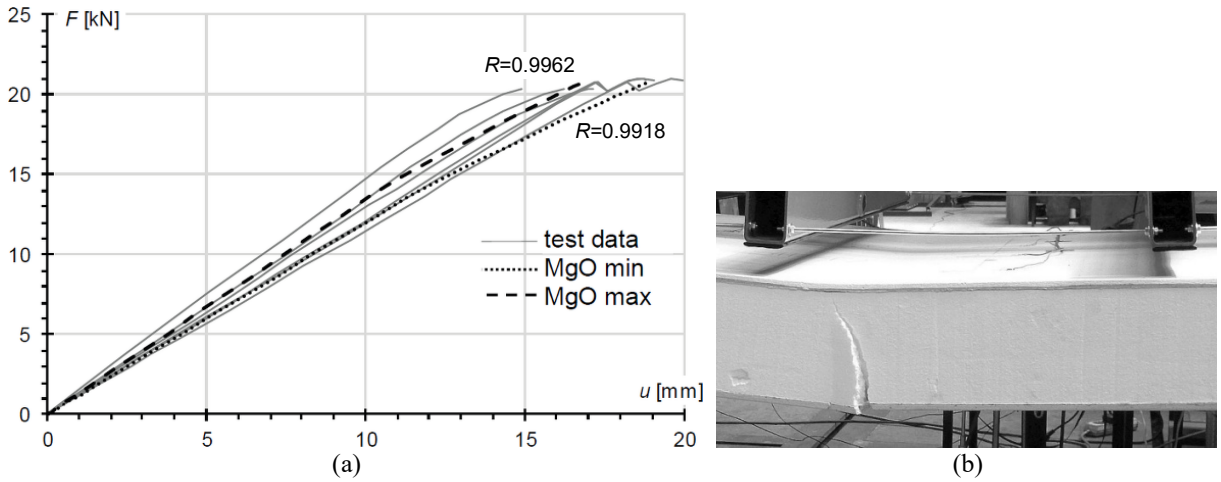

FIGURE 6. CSIP bending results: (a) comparison of numerical and test curves, R – correlation coefficient, (b) failure mode

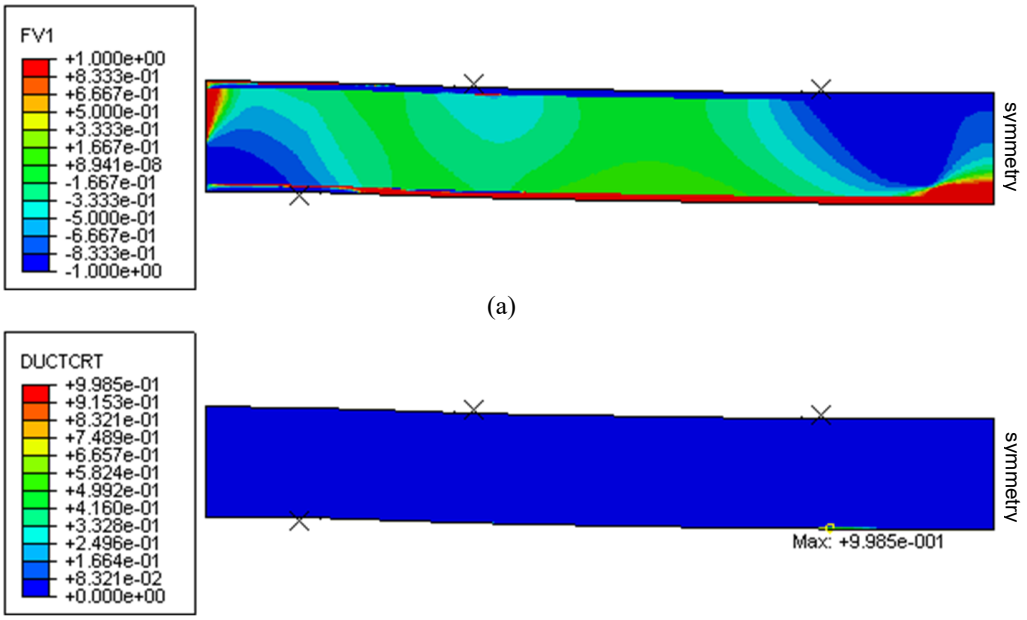

FIGURE 7. CSIP bending simulation map results: (a) state variable distribution, (b) damage initiation criterion

State variable distribution map (Fig. 7a) shows that user-defined procedure predicts the arrangement of material regions under compression and tension in a realistic manner. It automatically assigns appropriate parameter values to each integration point in accordance with Tab. 1. Material properties corresponding to state variables other than characteristic values presented in Tab. 1 are obtained automatically from linear interpolation. Comparison of numerical curves with averaged test results gives correlation coefficient values close to unity (Fig 6a), which means a very good compatibility. Damage criterion is fulfilled in an area on lower facing, near panel's axis of symmetry (Fig. 7b) which corresponds well with failure mechanism observed in the test (Fig. 6b).

Furthermore, a comparison of mid-span deflection in elastic range obtained from analytical formulae [2] was performed. Results were compared for a load level of 13 kN, a value for which both tested panels' response is clearly linear. A value of mid-span deflection averaged from the test data is 10.21 mm and vertical displacements obtained from numerical model for lower and upper limits of MgO board properties are 10.82 mm and 9.64 mm respectively, resulting in relative difference values of 5.9% and 5.6%. Since the analytical model requires assigning a single value for the modulus of elasticity within each layer [2] several sets of material parameters were considered; only values for EPS of density of 15 kg/m^3 (the core material used in tested CSIPs) were taken into account. Isotropy of all layers were assumed, resulting in core shear modulus $G_c = E_c/[2(1 + \nu_c)]$. Poisson number values for facings and core were 0.18 and 0.09 respectively. Mid-span deflections and difference values relative to averaged test results are presented in Tab. 2. Analytical results show much greater variance from the test data than results obtained from the proposed FEM model. The main reason behind this is that a reliable use of analytical equations requires determining an effective value of core shear modulus in a sandwich sample bending test [4, 7–9], while the presented numerical model operates on core material properties obtained from uniaxial compression and tension tests. Another factor is the dependency of MgO board's elastic properties on the stress state (different values in compression and tension) [20], which makes determining a single, effective value of both facings' modulus of elasticity a difficult task.

TABLE 2. Analytical model results in elastic range; subscripts: *f* – facing, *c* – core

	MgO board min		MgO board avg		MgO board max	
	EPS comp	EPS tens	EPS comp	EPS tens	EPS comp	EPS tens
E_f [MPa]	2430	2430	5235	5235	8040	8040
E_c [MPa]	5	7.2	5	7.2	5	7.2
u [mm]	14.05	11.32	11.29	8.57	10.45	7.74
difference [%]	37.6	10.8	10.5	16.1	2.3	24.2

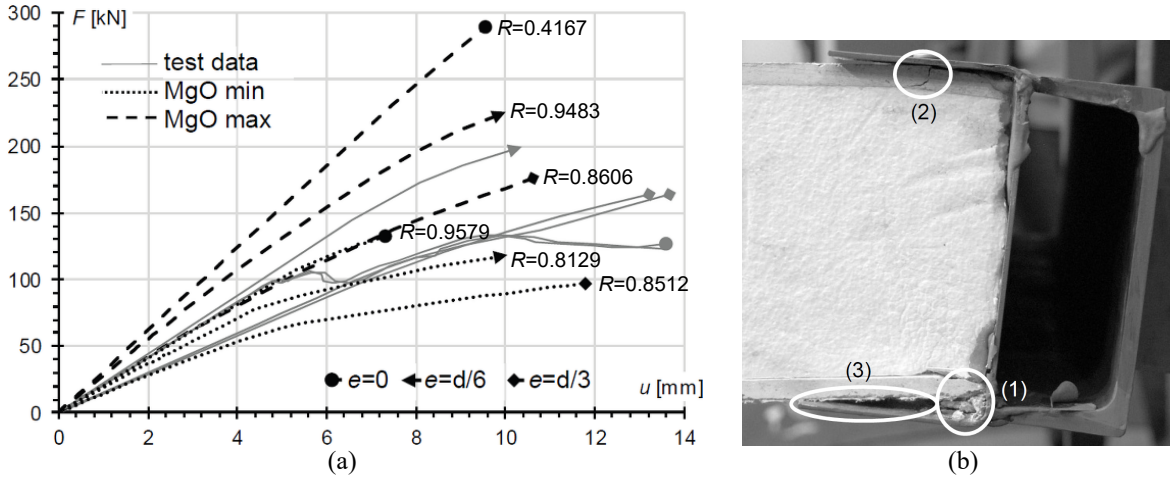

FIGURE 8. CSIP compression results: (a) comparison of numerical and test curves, R – correlation coefficient, (b) failure mode

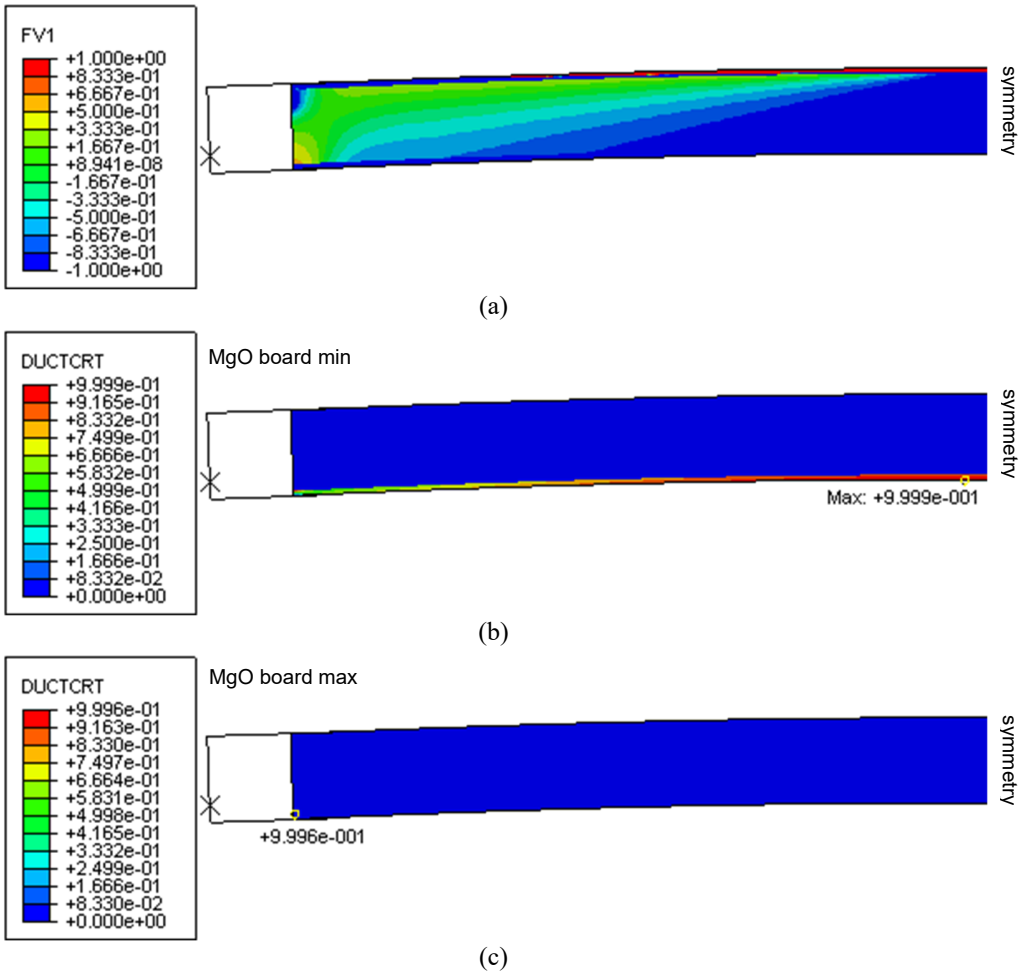

FIGURE 9. CSIP compression ($e = d/3$) simulation map results: (a) state variable distribution, (b) damage initiation criterion for lower limit MgO board properties, (c) damage initiation criterion for upper limit MgO board properties

Three CSIPs were subjected to edgewise compression with different values of the load eccentricity: $e = 0$, $e = d/6$ and $e = d/3$ (d in accordance with Fig 1) [27, 36]. Figure 8a, presenting comparison of force – compression curves, shows that laboratory test results fit well within the numerical prediction range in both curve shapes and failure loads. The model was even able to predict the premature failure of the panel submitted to uniaxial compression, which coincides with the lower limit of MgO board compression strength properties. The numerically obtained curves indicate that the failure load is decreasing with the increase of the eccentricity value, as expected.

Numerical result maps for all three eccentricities had similar characteristics, and therefore only one, most representative set is presented (Fig. 9). State variable distribution shows that though most of the numerical sample is under compression, there is a region under tension forming in upper facing, resulting from flexural deformation caused by high eccentricity value. Two different failure modes were observed for extreme MgO board properties – one initiated in mid-span (Fig. 9b) the other at the facing's edge. In laboratory tests only the second mode was observed (Fig. 8b). This is caused by FEM model idealisation, actual panel edges are especially prone to flaws appearing during transportation and structure assembly and it is nearly certain that is where the failure will initiate.

CONCLUSIONS

The final model validation by a comparison with the full-scale tests gave results that are satisfactorily consistent with the experimental data, both in terms of the nature of the curves obtained and the observed mechanisms of failure. The model allows for a prediction of full-scale CSIP failure modes, based on appropriate small-scale test data. This is mostly thanks to the user-defined procedure allowing defining a single material description which adjusts itself to appropriate stress state during analysis, regardless of sample geometry or loading type.

The FEA allowed identifying clear facing compression failure criterion, independent of sample's geometry. Facing failure in tension proved to be more problematic, different damage initiation parameters had to be used for samples of different geometries (Fig. 10). It is highly probable, that part of the reason is the size effect, but further model refinement is required to rule out other factors.

Additional small-scale tests required for the model refinement would need to include local strain measurement. This in turn would also give more insight into the matter of local, conditional strengthening of core – facing interface used to obtain correct failure modes.

The presented research shows, that using averaged properties for EPS foam of given density gives satisfactory results, however significant dispersion of values for MgO board makes such approach unreliable. Upper and lower limits were used instead in present analysis, resulting in numerical result spectrum rather than a single curve. In future research a reliability problem will be formulated and a solution based on the Response Surface Methodology [37] will be pursued.

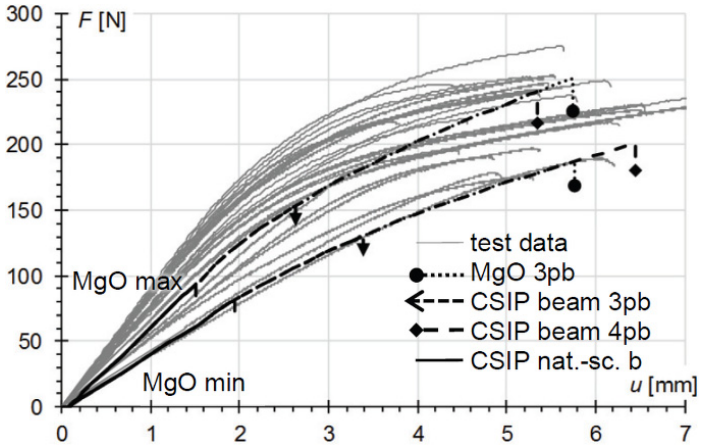

FIGURE 10. Comparison of force – displacement curves in MgO board bending for different tensile failure parameter values

ACKNOWLEDGMENTS

This work is dedicated to the memory of Professor Liviu Librescu (1930-2007) 10 years after his heroic death in the violent shooting at the Virginia Tech University on April 16, 2007.

REFERENCES

1. L. Alameda, V. Calderón, C. Junco, A. Rodríguez, J. Gadea and S. Gutiérrez-González, Materiales de Construcción **66**(324), e100 (2016).
2. H. G. Allen, *Analysis and design of structural sandwich panels*, edited by B.G. Neal (Pergamon Press, London, 1969).
3. R. Studziński, Z. Pozorski and A. Garstecki, Journal of Theoretical and Applied Mechanics **47**(3), pp. 685–699 (2009).
4. R. Studziński, Z. Pozorski and A. Garstecki, Journal of Constructional Steel Research **104**, pp. 227–234 (2015).
5. J. Pozorska, Z. Pozorski and Ł. Janik, Journal of Applied Mathematics and Computational Mechanics **16**(2), pp. 113–121 (2017).
6. J. Pozorska and Z. Pozorski, Procedia Engineering **177**, pp. 168–174 (2017).
7. M. Chuda-Kowalska and M. Malendowski, "Sensitivity analysis of behavior of sandwich plate with PU foam core with respect to boundary conditions and material model", *Advances in Mechanics: Theoretical, Computational and Interdisciplinary Issues*, The 3rd Polish Congress of Mechanics & 21st International Conference on Computer Methods in Mechanics Proceedings, edited by M. Kleiber *et al*. (CRC Press, London, 2016), pp. 125–128.
8. M. Chuda-Kowalska and M. Malendowski, Journal of Applied Mathematics and Computational Mechanics **15**(3), pp. 15–25 (2016).
9. M. Chuda-Kowalska, Z. Pozorski and A. Garstecki, "Experimental Determination of Shear Rigidity of Sandwich Panels with Soft Core", *Modern Building Materials, Structures and Techniques*, The 10th International Conference Proceedings (Vilnius Gediminas Technical University, Vilnus, 2010), pp 56–63.
10. W. Chen and H. Hao, Materials and Design **60**, pp. 409–423 (2014).
11. W. Chen, H. Hao, S. Chen and F. Hernandez, Materials and Design **84**, pp. 194–203 (2015).
12. W. Chen, H. Hao, D. Hughes, Y. Shi, J. Cui and Z.-X. Li, Materials and Design **69**, pp. 170–180 (2015).
13. M. Kujawa and C. Szymczak, Thin-Walled Structures **75**, pp. 43–52 (2014).
14. U. Caliskan and M. K. Apalak, Composites Part B **112**, pp. 158–175 (2017).
15. A. Kayello, H. Ge, A. Athienitis and J. Rao, Building and Environment **115**, pp. 345–357 (2017).
16. C. Borsellino, L. Calabrese and A. Valenza, Composites Science and Technology **64**, pp. 1709–1715 (2004).
17. M. A. Mousa and N. Uddin, Advanced Composite Materials **20**, pp. 547–567 (2011).
18. M. A. Mousa and N. Uddin, Materials and Design **32**, pp. 766–772 (2011).
19. M. A. Mousa and N. Uddin, Engineering Structures **41**, pp. 320–334 (2012).
20. A. Manalo, Construction and Building Materials **41**, pp. 642–653 (2013).
21. A. Mostafa, K. Shankar and E. V. Morozov, Applied Composite Materials **21**, pp. 661–675 (2014).
22. M. Miśkiewicz, K. Daszkiewicz, T. Ferenc, W. Witkowski and J. Chróścielewski, "Experimental tests and numerical simulations of full scale composite sandwich segment of a foot- and cycle- bridge", *Advances in Mechanics: Theoretical, Computational and Interdisciplinary Issues*, The 3rd Polish Congress of Mechanics & 21st International Conference on Computer Methods in Mechanics Proceedings, edited by M. Kleiber *et al*. (CRC Press, London, 2016), pp. 401–404.
23. M. Miśkiewicz, Ł. Pyrzowski, J. Chróścielewski and K. Wilde, "Structural Health Monitoring of Composite Shell Footbridge for Its Design Validation", *2016 Baltic Geodetic Congress (BGC Geomatics)*, (IEEE, New York, 2016), pp. 228–233.
24. J. Chróścielewski, M. Miśkiewicz, Ł. Pyrzowski, B. Sobczyk and K. Wilde, Composites Part B **126**, pp. 153–161 (2017).
25. Dassault Systèmes, Abaqus Analysis User's Manual, Providence, RI, USA, 2010, see https://www.3ds.com/.
26. A. Wawrzynowicz, M. Krzaczek and J. Tejchman, Archives of Acoustics **39**(3), 351–364 (2014).
27. Ł. Smakosz and J. Tejchman, Materials and Design **54**, pp. 1068–1082 (2014).

28. Ł. Smakosz and I. Kreja, “Experimental and numerical evaluation of mechanical behaviour of composite structural insulated panels”, *Recent Advances in Computational Mechanics*, 20th International Conference on Computer Methods in Mechanics Proceedings, edited by T. Łodygowski *et al*. (CRC Press, London, 2014), pp. 269–276.
29. Y. Frostig, Composite Structures **24**, pp. 161–169 (1993).
30. O. T. Thomsen and Y. Frostig, Composite Structures **37**(1), pp. 97–108 (1997).
31. M. Bischoff and E. Ramm, International Journal of Solids and Structures **37**, pp. 6933–6960 (2000).
32. L. Librescu and T. Hause, Composite Structures **48**(1–3), pp. 1–17 (2000).
33. I. Kreja, Central European Journal of Engineering **1**(1), pp. 59–80 (2011).
34. S. J. Salami, M. Sadighi and M. Shakeri, Journal of Sandwich Structures and Materials **16**(6), pp. 633–668 (2014).
35. L. L. Mercado and D. L. Sikarskie, Mechanics of Composite Materials and Structures **6**, pp. 57–67 (1999).
36. Ł. Smakosz and I. Kreja, “Experimental and numerical evaluation of mechanical behaviour of composite structural insulated wall panels under edgewise compression”, *Advances in Mechanics: Theoretical, Computational and Interdisciplinary Issues*, The 3rd Polish Congress of Mechanics & 21st International Conference on Computer Methods in Mechanics Proceedings, edited by M. Kleiber *et al*. (CRC Press, London, 2016), pp. 547-550.
37. K. Winkelmann and J. Górski, Journal of Theoretical and Applied Mechanics **52**(4), pp. 1019–1032 (2014).